



Received: 31 May 2019
Accepted: 22 July 2019
First Published: 30 July 2019

*Corresponding author: Kudzanayi Chiteka, Department of Industrial and Manufacturing Engineering, Harare Institute of Technology, Belvedere, Harare, Zimbabwe
E-mail: tavakudzira@gmail.com

Reviewing editor:
Duc Pham, School of Mechanical Engineering, University of Birmingham, United Kingdom

Additional information is available at the end of the article

MECHANICAL ENGINEERING | RESEARCH ARTICLE

Numerical investigation of installation and environmental parameters on soiling of roof-mounted solar photovoltaic array

Kudzanayi Chiteka^{1*}, S. N. Sridhara² and Rajesh Arora²

Abstract: A study of dust deposition on solar photovoltaics as influenced by the installation tilt angle, azimuth angle and the dust particles sizes was carried out. A 3-dimensional Computational Fluid Dynamics (CFD) simulation model was used with the Shear Stress Transport k- ω turbulence model being employed for wind flow analysis and discrete phase model was used for dust motion prediction. Response surface modelling was used to analyse the relationships between the installation parameters, dust particle sizes and dust deposition. The investigation revealed that in a 3-dimensional simulation, the influence of tilt angle is almost similar to the effect of azimuth angle for multi-storey rooftop photovoltaic arrays. Dust particle size of 100 μm had the most deposition resulting in more soiling compared to the 10 μm size dust particles. Soiling of roof-mounted solar PV modules is less on multi-storey building installations compared to ground-mounted solar PV arrays which experienced 13% more deposition. Manipulation of the installation azimuth and tilt angles on roof-mounted installations can be effectively used for soiling minimisation.

ABOUT THE AUTHORS

Kudzanayi Chiteka is a lecturer in the Department of Industrial and Manufacturing Engineering at Harare Institute of Technology. He is a research scholar in solar energy at Amity University, Gurgaon, India. His research interests are renewable energy systems and technology.

S. N. Sridhara is working as a Professor in Mechanical Engineering Department, Amity University Haryana, Gurgaon. He received his doctorate and master's degree from IISc Bangalore. His areas of expertise are solar photovoltaics, spray formation, heat transfer, computational fluid dynamics, thermal & fluid engineering and hybrid vehicles.

Dr. Rajesh Arora is working as an Associate Professor in Mechanical Engineering Department, Amity University Haryana, Gurgaon. He received his doctorate degree from YMCA UST, Faridabad and Masters from IIT, Delhi. His areas of expertise are solar photovoltaics, energy and exergy analysis of thermal systems, heat transfer, computational fluid dynamics, multi-objective optimization and decision making.

PUBLIC INTEREST STATEMENT

Solar energy derived from the sun has found many uses including power generation water heating and space heating. However, the issue of soiling can be a deterrent factor to the wider adoption of solar energy. Soiling reduces the amount of irradiance converted into useful energy due to its shading effect. It is therefore technically and economically justifiable to develop new ways of mitigating the negative effects of soiling to allow maximum utilisation of the installed capacity of the solar collectors. For rooftop solar photovoltaics, cleaning is more difficult and hence there is a need to develop mitigation strategies that take advantage of the natural cleaning mechanisms such as wind and rain. This study seeks to evaluate and analyse the soiling characteristics of different installation configurations on a rooftop photovoltaic array. Further, the configurations and variables, which give the maximum and minimum soiling, are identified and analysed.

Subjects: Mechanical Engineering; Power & Energy; Clean Technologies; Renewable Energy

Keywords: Photovoltaic array; dust deposition; modelling; installation configuration; CFD simulation; soiling parameters

1. Introduction

Solar photovoltaic (PV) energy is among the preferred alternative energy sources due to its abundance and renewable nature. In the past ten years, there has been a 50% average increase in the global PV market (Connolly, Lund, Mathiesen, & Leahy, 2010) and by year 2019, about 112 GW global solar PV demand is anticipated (Enkhardt, 2018). However, the wider adoption of solar PV energy can be slowed down due to the influence of soiling which is the accumulation of dust and other foreign materials on a solar PV module surface (Sarver, Al-Qaraghuli, & Kazmerski, 2013; Tanesab, Parlevliet, Whale, & Urme, 2019). The influence of soiling on solar PV arrays can have drastic effects (Mussard & Amara, 2018; Said, Hassan, Walwil, & Al-Aqeeli, 2018). For example, Adinoyi and Said (2013) reported a soiling power loss of 50% in Saudi Arabia while losses ranging from 5%–70% were also recorded in different places with varying climatic conditions and time of exposure (Adinoyi & Said, 2013; El-Nashar, 1994; Pavan, Mellit, De Pieri, & Kalogirou, 2013). A study in Saudi Arabia revealed a 32% decrease in PV power efficiency due to soiling after several months of exposure (El-Nashar, 1994). A different study by Pavan et al. (2013), reported annual power losses between 1% and 5% for poly-crystalline PV collectors. Soiling is therefore a phenomenon which is dependent on the place of occurrence and the time of exposure.

There are several variables influencing soiling and these were investigated in different researches. The influence of dust particle sizes on soiling was studied by El-Shobokshy and Hussein (1993) and it was reported that small particles have more detrimental effects compared to larger-sized particles. The influence of wind speed was also considered in solar PV soiling studies. An investigation by Said et al. (2018) indicated that the influence of wind velocity on solar PV module performance is dependent on its speed and direction. A different study evaluated the effect of wind speed on dust deposition and higher wind speeds were reported to cause more soiling (Goossens & Kerschaefer, 1999). However, other studies on wind speed reported otherwise (Maghami et al., 2016; Mani & Pillai, 2010).

The installation configuration, i.e. the tilt angle and azimuth angle also affect dust deposition on solar PV module. The effects of tilt angles on soiling were investigated and it was reported that higher tilt angles have lower soiling rates compared to lower tilt angles (Elminir et al., 2006; Mekhilef, Saidur, & Kamalisarvestani, 2012). Further studies on the influence of tilt angles on soiling were performed by Xu et al. (2017) and a model relating the tilt angle and dust deposition density was developed and integrated into the PV output model. Investigations on the influence of installation azimuth indicated that surfaces facing away from the wind experience less soiling compared to the surfaces facing the direction of wind flow (Goossens, Offer, & Zangvil, 1993; Mailuha, Murase, & Inoti, 1994; Mani & Pillai, 2010). The azimuth angle of a solar PV surface is the angle between a line due south passing through the PV module and the horizontal projection of the normal to the PV surface. A study to evaluate the influence of installation tilt, azimuth and height on ground-mounted PV modules was carried out by Chiteka, Arora, and Jain (2019) and it was reported that tilt angle is more influential on dust deposition compared to azimuth for heights of installation between 1 m and 5 m.

Simulations and experimental investigations were performed on particle deposition characteristics on surfaces including solar PV modules. Particle adhesion characteristics were reported to be dependent on impact velocity of the particle onto the surface for both normal and oblique impact (Li, Dunn, & Brach, 2000). A general study by Klinkov, Kosarev, and Rein (2005) developed a method to determine the fate of a particle on impact with a surface based on its impact velocity and particle diameter.

A limited number of simulation studies in dust deposition on solar PV collectors were reported in literature. For example Lu, Lu, and Wang (2016) performed a numerical investigation of dust

deposition on an isolated building-mounted solar PV array. The study revealed that smaller sized particles of 10 μm had more deposition compared to 50 μm sized particles. In another study, Lu and Zhang (2018) studied the dry deposition by Computational Fluid Dynamics (CFD) simulation of mono-disperse and polydisperse dust on rooftop PV collectors and reported no distinction between mono-disperse and polydisperse dust deposition characteristics. Deposition characteristics on ground-mounted PV collectors were also investigated and a 13.71% deposition rate was recorded on 100 μm sized dust at a velocity of 1.3m/s while a deposition rate of 14.28% was recorded on 150 μm dust particles at a velocity of 2.6m/s (Lu & Zhao, 2019). Dust deposition characteristics on ground-mounted multi-row solar PV installations was investigated using CFD simulation and the study reported 13.18% more deposition on front rows compared to the rear rows (Lu & Zhang, 2019). Further, large-sized dust particles deposited more on the front rows and smaller sized particles settled on the rear rows.

In another study by Heydarabadi, Abdolzadeh, and Lari (2017), the influence of varying tilt angles, wind direction, dust concentration and particle size was evaluated using CFD on ground-mounted PV modules. The results showed that different particle sizes have different deposition characteristics. Further, it was found that higher wind speeds require higher tilt angles for maximum deposition.

Soiling mitigation of soiled solar PV systems is of utmost importance in solar PV power generation. However, studies indicate that the size of the solar PV array and the height of the building contribute to the complexity and tediousness experienced in soiling mitigation (Kumar, Sudhakar, Samykano, & Sukumaran, 2018). The cleaning of PV installations on high rise buildings is complex and expensive as it requires specialised pumping of cleaning water (Williams, n.d.). Further, the existing robots are difficult to employ on building integrated and building applied PV arrays as these robots are designed for open space PV installations (Kumar et al., 2018).

The use of novel dust mitigation procedures such as electrodynamic shield, electrostatic cleaning, super hydrophilic and superhydrophobic coatings was found to yield positive results (Chen, Chesnutt, Chien, Guo, & Wu, 2019; Guo, Javed, Khoo, & Figgis, 2019; Kawamoto & Guo, 2018; Mozumder, Mourad, Pervez, & Surkatti, 2019; Wang et al., 2018), however, their use has not received wider application to date. Further, literature has revealed that although a number of approaches exist, there is no one clear approach to soiling mitigation and the economic feasibility of these approaches need further consideration (Said et al., 2018).

Although CFD simulations have been performed on soiling of solar PV collectors, these were mainly focused on single storey rooftop and ground-mounted PV collectors (Heydarabadi et al., 2017; Lu et al., 2016; Lu & Zhang, 2018, 2019; Lu & Zhao, 2019). The present study focuses on simulation studies on soiling of PV arrays mounted on multi-storey buildings which is scarce in literature. The wind profiles and dust deposition characteristics on ground-mounted photovoltaics and single-storey mounted photovoltaics is different to that on a multi-storey building. Wind flow profiles on PV collectors mounted on a single storey building are influenced by the roof characteristics such as its inclination. However, on a multi-storey building, both inclined and flat roofs are common and a different mounting structure is normally used. The use of a different mounting structure and the height of multi-storey buildings makes wind flow characteristics different and more complex.

The cleaning mechanism required on ground-mounted and single-storey rooftop PV modules is simpler and different to that required on a multi-storey rooftop-mounted photovoltaic array. The cleaning equipment normally used for ground-mounted and single-storey buildings usually traverses on the ground while this is inapplicable to multi-storey buildings which require specialised equipment and water pumping. Citing this difficulty, it is therefore important to evaluate and analyse the factors affecting dust deposition on a multi-storey building and take advantage of natural cleaning agents such as wind and rain. Soiling mitigation methods that can utilise the natural cleaning agents such as rain and wind are important for immediate application in the short term and thus need to be explored extensively. Arora and Arora (2018) accomplished energy and exergy investigations on 1 kW installed rooftop SPV plant in Northern India. Further, Arora, Arora,

and Sridhara (2019) carried out performance assessment of 186 kWp power plant in Northern India. The SPV systems can also be integrated with various energy conversion systems viz. Stirling heat engines in view of fabricating a hybrid system. (Arora, Kaushik, & Kumar, 2016a, 2016b, 2017).

The effects of installation tilt and azimuth angle as well as the dust particle sizes on both ground mounted and multi-storey building were investigated in this study and a comparative analysis was also carried out. Literature has indicated that 3-dimensional CFD simulation of dust deposition on solar photovoltaics is still limited. Azimuth is important in dust deposition studies on a PV array because it influences wind flow characteristics and the effective area of exposure to dust deposition. It is therefore required to evaluate and analyse the effects of the installation tilt, azimuth as well as the influence of high rise building installations on dust deposition. These factors motivated the investigators to take up the current investigation.

This study is organized as follows: Section 1 outlines the introduction, which also consists of the literature review leading to the identified area of research. Section 2 discusses the materials and methods employed in this study. Section 3 has the results and discussions of the outcomes of the CFD investigation, and lastly, section 4 gives the conclusion of this investigation.

2. Numerical methodology

2.1. Experimental design

A full factorial face centred central composite experimental design was employed in the design of experiments and a total of 27 simulation experiments were conducted. Parameters including tilt, azimuth and dust particle size were investigated at a constant wind speed of 5m/s. The tilt angle was varied between 5° and 30° while azimuth was varied between 0° and 22.5°. In this study, the azimuth angle was measured with respect to North where 0° means 0° North. The azimuth and tilt angles were selected within the acceptable limits that do not significantly affect the solar radiation incident on the solar PV module. Calcium carbonate dust particles with a density of 2800 kg/m³ were used in this study. Dust particle sizes were studied in the range 10 µm to 100 µm. Table 1 outlines the parameters used in this study.

2.2. Fluid flow and turbulence modelling

The Reynolds Averaged Navier Stokes (RANS) governing equations were used in fluid flow analysis. Turbulence modelling was performed using the Shear Stress Transport (SST) k- ω turbulence model. This model was used due to its better performance compared to other turbulence models on dust deposition applications (Karava, Jubayer, & Savory, 2011; Lu & Zhao, 2019). Dust motion tracking was performed using the Discrete Phase Model (DPM) and particle-particle interactions were ignored. The DPM was employed due to its suitability in modelling two-phase flow problems consisting of a single continuous phase and a discrete phase with a negligible volume fraction of less than 12%. In this DPM modelling, particle-particle interactions were considered negligible and the existence of the suspended particles did not affect fluid flow field (Zhu, Li, & Wang, 2018). The Discrete Random Walk model (DRW) was utilised in modelling the turbulent dispersion of particles for accurate prediction of deposition behaviour of dust particles.

The fluid flow was analysed using RANS governing equation (Equation 1) (Heydarabadi et al., 2017) which describes the relationship between velocity, pressure, temperature and density. The RANS

Table 1. Experimental parameters

Parameter	Low	Medium	High
Tilt (°)	5	17.5	30
Azimuth (°)	0	11.25	22.5
Dust size (µm)	10	55	100

equations used are based on laws of conservation of mass, momentum, and energy. These are shown by Equations 2–4 (Heggøy, 2017). Where; ρ (kg/m^3), \mathbf{u} ($\text{m}\cdot\text{s}^{-1}$) and κ ($\text{Wm}^{-1}\text{K}^{-1}$) are, respectively, density, velocity vector and thermal conductivity while t (seconds), Φ , and $\Gamma_{\phi,\text{eff}}$ (m^2/s) represent time, the independent flow variable and the effective diffusion coefficient. S_ϕ ($\text{kg/m}^3\text{s}$) is the source term.

$$\rho \frac{\partial \bar{\phi}}{\partial t} + \rho \bar{u}_j \frac{\partial \bar{\phi}}{\partial x_j} - \frac{\partial}{\partial x_j} \left[\Gamma_{\phi,\text{eff}} \frac{\partial \bar{\phi}}{\partial x_j} \right] = S_\phi \quad (1)$$

$$\frac{\partial \rho}{\partial t} + \nabla \rho \mathbf{u} = 0 \quad (2)$$

$$\rho \frac{D\mathbf{u}_i}{Dt} = -\frac{\partial p}{\partial x_i} + \frac{\partial}{\partial x_j} \left[\mu \left(\frac{\partial u_i}{\partial x_j} + \frac{\partial u_j}{\partial x_i} - \frac{2}{3} \frac{\partial u_r}{\partial x_r} \delta_{ij} \right) \right] + \rho F_i \quad (3)$$

$$\rho \frac{De}{Dt} = -\rho \frac{\partial u_i}{\partial x_j} + \frac{\partial u_i}{\partial x_j} \mu \left(\frac{\partial u_i}{\partial x_j} + \frac{\partial u_j}{\partial x_i} - \frac{2}{3} \frac{\partial u_r}{\partial x_r} \delta_{ij} \right) + \frac{\partial}{\partial x_i} \left(\kappa \frac{\partial T}{\partial x_i} \right) \quad (4)$$

The formulation of the SST k - ω turbulence model used is shown in Equations 5 and 6 (Zhao, Zhang, Li, Yang, & Huang, 2004). Where; \tilde{G}_k and \tilde{G}_ω respectively represent the generation term for turbulent kinetic energy k (m^2/s^2), and the generation term for specific dissipation rate. ω (s^{-1}). Γ_ω and Γ_k are the effective diffusivity of ω and k . User-defined source terms N_k and N_ω are taken as zero in this study while K_ω is the cross-diffusion term.

The SST k - ω turbulence model exhibit the best of k - ϵ and k - ω two-equation models (Lee, Wray, & Agarwal, 2016). Such a model simplifies the prediction of the commencement and amount of flow separation occurring at adverse pressure gradients.

$$\frac{\partial}{\partial t} (\rho k) + \frac{\partial}{\partial x_i} (\rho k u_i) = \frac{\partial}{\partial x_j} \left(\Gamma_k \frac{\partial k}{\partial x_j} \right) + \tilde{G}_k - L_k + N_k \quad (5)$$

$$\frac{\partial}{\partial t} (\rho \omega) + \frac{\partial}{\partial x_i} (\rho \omega u_i) = \frac{\partial}{\partial x_j} \left(\Gamma_\omega \frac{\partial \omega}{\partial x_j} \right) + \tilde{G}_\omega - L_\omega + K_\omega + N_\omega \quad (6)$$

2.3. Dust deposition and dust motion modelling

Motion of dust particles was predicted using the DPM model and the formulation of such a model is shown in Equations 7 and 8 (Heydarabadi et al., 2017). The wind-dust particles interaction was considered in the CFD numerical computation. In this investigation, however, dust particle to particle interactions were considered insignificant because the dust concentration in the fluid air was considered as dilute. In the CFD simulation, forces including drag force, gravitational force, and thermophoresis were accounted for.

$$\frac{\partial \mathbf{x}_j^p}{\partial t} = \mathbf{u}_j^p \quad (7)$$

$$\frac{\partial \mathbf{u}_j^p}{\partial t} = \frac{1 + 0.15 \text{Re}_d^{0.687}}{\tau_p} (\mathbf{u}_j^f - \mathbf{u}_j^p) + \left(1 - \frac{1}{S} \right) \mathbf{g}_i \quad (8)$$

Where; $\mathbf{u}_j^f = \bar{\mathbf{u}}_i + \mathbf{u}_j'$; \mathbf{u}_j' is the mean flow at the particle's position. t (s) is the time; \mathbf{u}_j^p (m/s) is centre velocity of particle; \mathbf{u}_j' (m/s) is velocity flow fluctuation; \mathbf{x}_j^p is the particle position; d is the diameter and S is the particle to fluid density ratio; \mathbf{g}_i (m/s^2) is the gravitational acceleration; $\text{Re} = |\mathbf{u}_j^f - \mathbf{u}_j^p| \frac{d}{\nu}$ is Particles' Reynolds number; The term, $\frac{1 + 0.15 \text{Re}_d^{0.687}}{\tau_p} (\mathbf{u}_j^f - \mathbf{u}_j^p)$ in Equation 8 is the Stokes drag and τ_p is the Stokes relaxation time and is given by $\tau_p = \frac{(Sd_p^2 C_c)}{18\nu}$ and the Stokes–Cunningham slip correction factor is given by C_c which modifies the exerted drag due to slip on very fine particles and is outlined in Equation 9. λ represents the mean free path of gas molecules in (μm) and d (cm) is the diameter of the dust particle in cm.

$$C_c = 1 + \frac{\lambda}{d} \left(2.514 + \frac{0.8}{e^{\frac{0.55d}{\lambda}}} \right) \quad (9)$$

The gravitational force in Equation 8 is given by $(1 - \frac{1}{5})g_i$. The DRW model was employed in modelling the turbulent dispersion of particles for accurate prediction of dust particle deposition behaviour (Zhao et al., 2004). Respective values of 0.5 and 0.55 were assumed for the roughness constants (C_s) for the PV module and the wall since the solar PV module surface is more uniform compared to the building wall. Moreover, roughness lengths z_o of, respectively, 0.0001 and 0.001 were used for the solar PV surface and the building wall and the formulation in Equation 10 was employed in determining the roughness height k_s for both the solar PV and the building wall (Liu et al., 2018; X. Zhang, 2009).

$$k_s C_s = 9.793 z_o \quad (10)$$

A constant wind velocity, U of 5m/s was used in this present study while the initial pressure was set as the standard atmospheric pressure. The wind speed at the solar PV height was determined using Equation 11 (Twidell & Weir, 2015) which describes the variation of wind speed with height where U_z is the wind velocity at height z , U is the characteristic speed, z_o is the roughness length and d is the zero plane displacement and its value is slightly less than the height of the local obstructions.

$$U_z = U \ln \left(\frac{z - d}{z_o} \right) \quad (11)$$

The inlet wind velocity and the Turbulent Kinetic Energy (TKE) profiles were compared to the results of an experimental investigation by Tominaga, Akabayashi, Kitahara, and Arinami (2015). The results are displayed in Figures 1 and 2 where $Z(m)$ represent the height from the ground in the computational domain at any particular location of interest, $h(m)$ is the PV module height, $U_h(m/s)$ is the velocity at PV module height and $K(m^2/s^2)$ is the turbulent kinetic energy. There was 0.25% and 0.38% difference between the results of the experiments by Tominaga et al. (2015) and the simulations, respectively, for the wind velocity profile at inlet and the Turbulent Kinetic Energy (TKE) profile.

2.4. Computational domain

The computational geometry used in this study was developed using ANSYS design Modeller 17. The schematic of the building model of a 3-storey building with an installed rooftop solar PV array is shown in Figure 3. The building had the following dimensions; length (L) = 20 m, width (W) = 15 m and height (H) = 10 m. The solar PV array installed had a total surface area of 24 m². The computational domain used by Abiola-Ogedengbe, Hangan, and Siddiqui (2015) in their wind tunnel experiments was mimicked in this study. Wind profile in such a computational domain resembled wind flow in open terrain. The present computational

Figure 1. Wind velocity profile at inlet. Experimental data was adopted from by Tominaga et al. (2015).

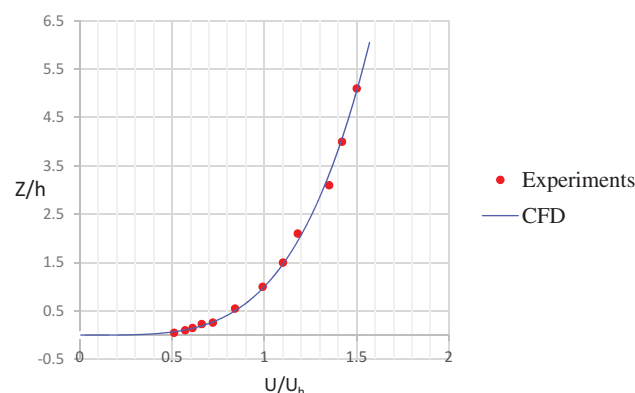


Figure 2. Turbulent kinetic energy (TKE) profile.
 Experimental data was adopted from by Tominaga et al. (2015).

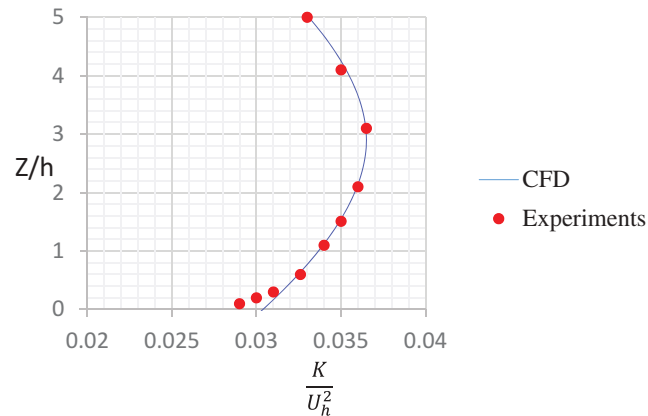
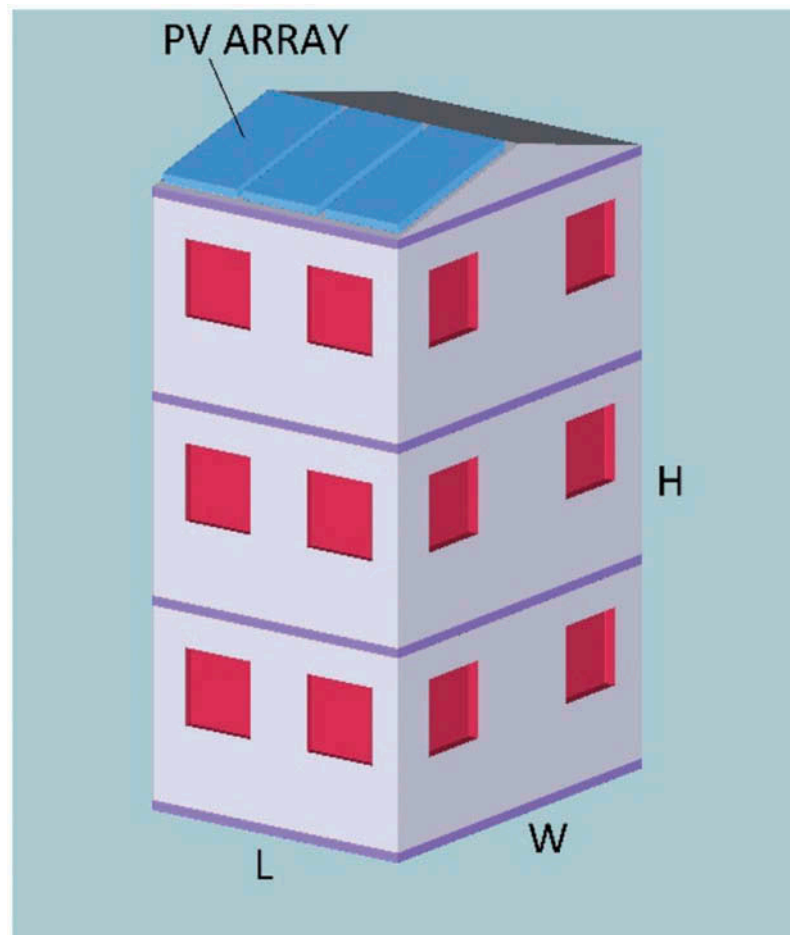


Figure 3. Schematic of the 3-storey building with a PV array installed.



domain was developed to produce the same mean pressure coefficient obtained in the study by Abiola-Ogedengbe et al. (2015).

The height (h) of installation of the PV module measured from the ground was given by $H + 0.5$ m thus $h = 10.5$ m. The length, height and width of the computational domain was given by $21.4h$, $6h$ and $9h$ respectively and this corresponds to 224.7 m, 63 m and 94.5m, respectively. A distance of $5h$ (52.5 m) was put between the computational inlet and the building while

a distance of $15h$ (157.5 m) was left between the rear of the building and the outlet of the computational domain. These dimensions were selected to make sure that there is no airflow obstruction on the solar PV collector by the channel wall boundary layers as shown in Figure 4.

2.5. Solution strategy

Resolving of the conservation equations of wind flow was done using the Finite Volume Method (FVM) and the SIMPLE (Semi-Implicit Method for Pressure Linked Equations) algorithm was used in decoupling the pressure and velocity fields. The second-order upwind scheme represented by Equation 12 (Tominaga et al., 2015) was used to discretize the diffusion and convection terms. The Runge-Kutta technique was used in resolving the motion equations of the dust particles. The solution convergence criteria of 10^{-6} for Residual Mean Square Error (RMSE) values was used for the fine mesh selected.

$$\phi_f, \text{SOU} = \phi + \nabla \phi \cdot \vec{r} \quad (12)$$

where ϕ_f , SOU and \vec{r} respectively represent the face value (using second-order upwind, SOU) and the displacement vector from the upstream cell centroid to the face centroid; ϕ & $\nabla \phi$ are the cell-centred value and its gradient in the upstream cell.

2.6. Grid independence study

Grid independence study was carried out to determine the minimum grid size that can give the best results. Three grids were tested and these were identified in the study as fine (628 435), medium (492 729) and coarse (152 964). For each mesh size, the number of particles collected on the solar PV collector was recorded and a comparative analysis was done on the different mesh sizes as shown in Figure 5. The results revealed that a fine grid was superior to other mesh sizes with a respective difference of 3.1% with the medium mesh and 17% with the coarse mesh. It was therefore concluded that a fine mesh would give the best results.

Simulations of airflow fields around the solar PV module were performed to evaluate solar PV soiling and validation of the simulations was done using Abiola-Ogedengbe et al. (2015) experimental results of wind tunnel experiments as shown in Figure 6, where w and W_p are, respectively,

Figure 4. Computational domain with boundary conditions.

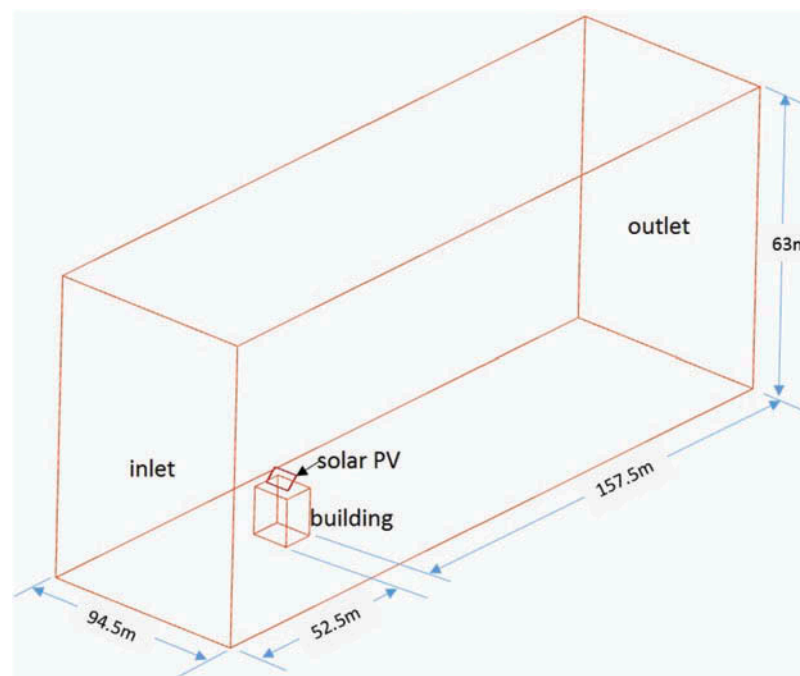


Figure 5. Grid independency study.

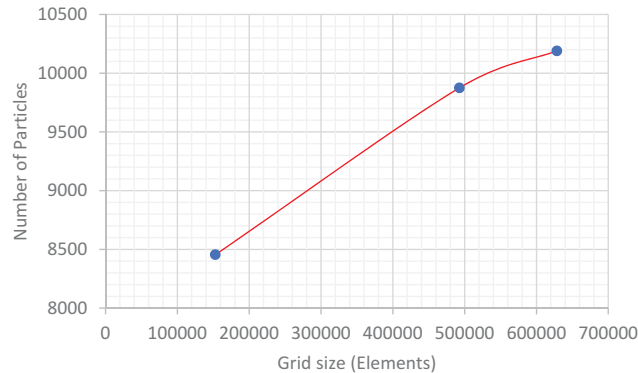
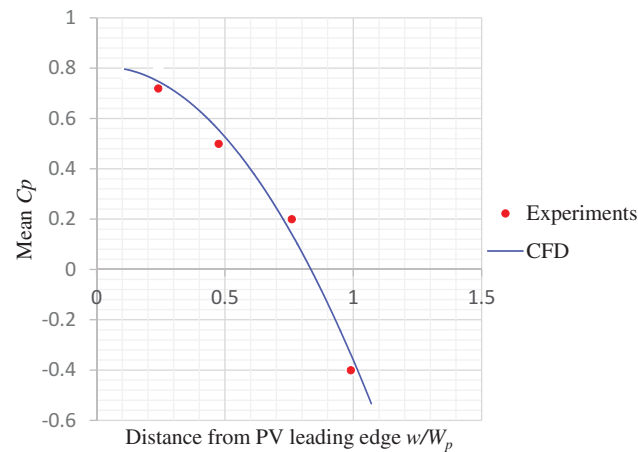


Figure 6. Experimental validation of the mean pressure coefficient (C_p).



the distance from the leading edge measured along the solar and the solar panel width. The pressure coefficient (C_p) profile of the simulation results correctly resembled the experimental results and hence it was concluded that the CFD simulation model was capable of accurately predicting the airflow fields near the PV module.

2.7. Insolation yield on varying azimuth angles

Annual insolation received by a tilted solar PV on different azimuth angles was computed using Angstrom's model for radiation on a tilted plane represented by Equation 13. \bar{H}_d , \bar{H}_b and K_T are respectively the diffuse irradiance, beam irradiance, and the clearness index. R_b , R_d and R_r are the tilt factors for beam, diffuse and reflected irradiance.

$$H_T = \bar{H}_b R_b + \bar{H}_d R_d + \bar{H}_g R_r \quad (13)$$

3. Results and discussions

3.1. Experimental design and dust deposition analysis

The influence of installation tilt and azimuth as well as the influence of dust particle sizes on soiling of solar photovoltaics was studied using CFD simulations. Simulation experiments amounting to 27 with varying tilt and orientation (wind direction) at a constant wind speed of 5m/s were performed and wind flow was predicted using the RANS equations. The SST k- ω turbulence model was employed in resolving wind flow turbulence near the solar PV collector. Dust particle trajectories were tracked using the DPM model while the DRW model predicted the turbulent dispersion.

Design of experiments was done using Design Expert v10.0. and Software Fluent v.17 was used in the simulation experiments. PVSyst v.6.70 was used in computation of the annual solar irradiance yield for the different azimuths used. The results of the solar irradiance yield for different azimuths at an optimised tilt angle of 23° for Harare, Zimbabwe are shown in Table 2. The percentage difference in energy yield between the optimum azimuth and azimuths of 157.5° and 202.5° was also computed. It was found that variation in azimuth angle by up to 22.5° yield a marginal loss in irradiance of up to an annual maximum of 0.69%. The simulation results of the designed experiments and CFD simulations are also highlighted in Table 3. Figure 7 gives the generated response surfaces used in analysing the contribution of the tilt, azimuth and dust particle sizes.

It is noted that the three parameters used in this study have an extent to which they affect dust deposition. In Figure 7, response surfaces are displayed showing the relationships between the different variables. The red dots indicate the design points above the predicted values of the quadratic model. The colour gradient from blue to red shows the region of increasing dust

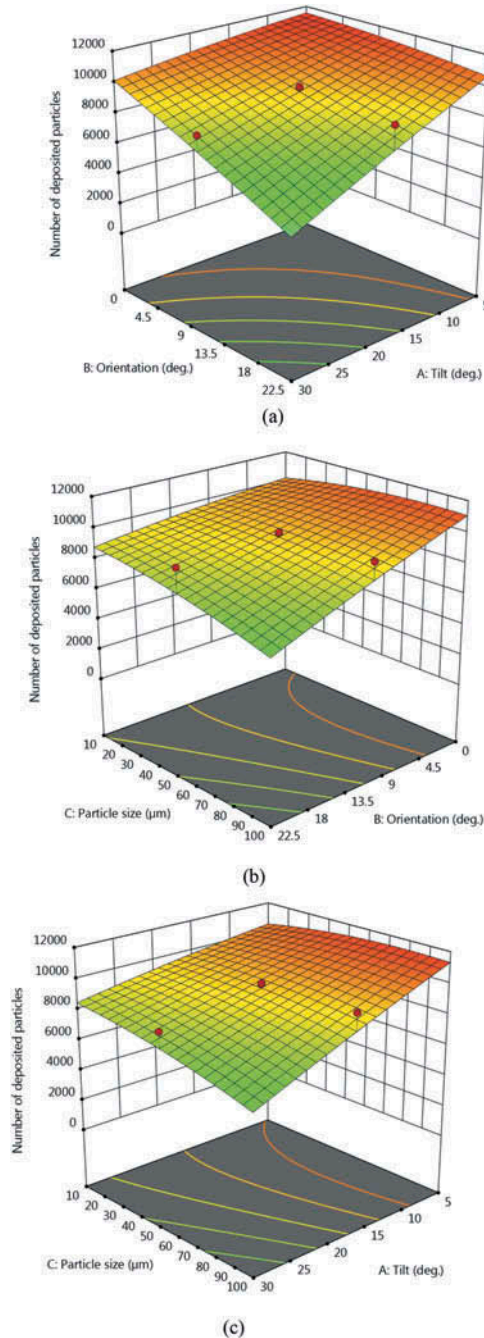
Table 2. Annual yield of solar irradiance at different azimuth angles

	Azimuth	Yield (kWh/m ²)	% difference
1	0.0°	2026	0
2	-22.5°	2015	0.54
3	22.5°	2012	0.69

Table 3. Experimental design and simulation results

Run	Factors			Response	
	Tilt (°C)	Azimuth (°C)	Particle size (µm)	Effective surface area of exposure (m ²)	Number of deposited particles on solar PV
1	5	0	10	24.00	11,500
2	5	0	100	24.00	11,890
3	5	11.25	55	23.54	10,720
4	5	22.5	100	22.17	10,290
5	5	22.5	10	22.17	10,000
6	17.5	0	55	24.00	9870
7	17.5	11.25	55	23.54	9650
8	17.5	11.25	10	23.54	8960
9	17.5	11.25	55	23.54	9500
10	17.5	11.25	55	23.54	9870
11	17.5	11.25	100	23.54	10,000
12	17.5	11.25	55	23.54	9650
13	17.5	11.25	55	23.54	8780
14	17.5	11.25	55	23.54	9000
15	17.5	22.5	55	22.17	9480
16	30	0	100	24.00	10,100
17	30	0	10	24.00	9620
18	30	11.25	55	23.54	8680
19	30	22.5	100	22.17	10,000
20	30	22.5	10	22.17	6980

Figure 7. Response surfaces for the accumulated particles with varying tilt, azimuth and dust particle sizes.



deposition where blue shows the region of low dust deposition and red is the region of high dust deposition. In Figure 7(a), it is shown that decreasing the tilt angle of the PV panel has an effect of increasing dust deposition. This is due to the effect of gravitational force having more influence on steeper gradients. It can therefore be concluded that tilt angle is inversely proportional to dust deposition a result which was also reported in other studies (Jiang, Lu, & Lu, 2016; Maghami et al., 2016; Mekhilef et al., 2012; Sayyah, Horenstein, & Mazumder, 2014). On the other hand, increasing the azimuth reduces dust deposition. This is because increasing the azimuth angle in relation to wind flow reduces the effective surface area for wind action on the PV collector. The reduction of soiling with wind flow direction agrees well with results reported in literature (Goossens et al.,

1993; Mailuha et al., 1994; Mani & Pillai, 2010). The results in Figure 7(a) also indicate the need for both low tilt and azimuth angle for maximum soiling. Huge amounts of soiling can also be obtained if either tilt angle or azimuth angle assumes a low value. Further, the results indicate that tilt and azimuth angles have almost equal contribution to soiling on PV installations on multi-storey building rooftops. However, tilt angle is slightly more influential compared to azimuth angle.

The results shown in Figure 7(b and c) show that dust particle sizes have a significant influence on dust deposition. However, its influence cannot be equated to that of either tilt or azimuth angle. It is shown that increase in dust particle size resulted in increasing rate of dust deposition with minimum deposition experienced on 10 μm dust particles while maximum deposition rate being recorded for the largest particles sizes of 100 μm . This result shows the differences in deposition characteristics between single-storey and multi-storey buildings. For example, a similar study on a single storey building by Lu et al. (2016) reported maximum deposition occurring at 10 μm particle size which is different for multi-storey buildings considered in the present study. The increase in deposition with increasing dust particle size was also reported in a different study by Lu and Zhao (2018).

The result shown in Figure 7(c) shows that the combination of a low tilt angle and large particle sizes results in higher deposition levels of the dust particles. Larger sized particles are more affected by the force of gravity and hence they tend to deposit more compared to smaller sized particles which may remain suspended in the fluid air for a longer period (Lu & Zhang, 2019; Lu & Zhao, 2018).

The parameters used in this study can be listed in order of their importance in soiling, respectively, as tilt angle, azimuth angle and dust particle size. However, there is only a small difference of 14.6% in the contribution of tilt angle compared to the contribution of azimuth angle. When compared to the previous studies by Chiteka et al. (2019) on ground-mounted PV modules, this present study indicates that the influence of tilt angle is significantly less when compared to ground-mounted PV modules. Parameter correlation analysis was performed and the results are shown in Table 4. There was an 11% decrease in the relevance of the tilt angle while, the influence of azimuth angle became more significant with its relevance increasing by 24% when compared to previous studies (Chiteka et al., 2019). This result indicated the importance of azimuth angle in soiling studies on rooftop PV modules on a multi-storey building.

3.2. Solar PV module wind flow fields and dust deposition

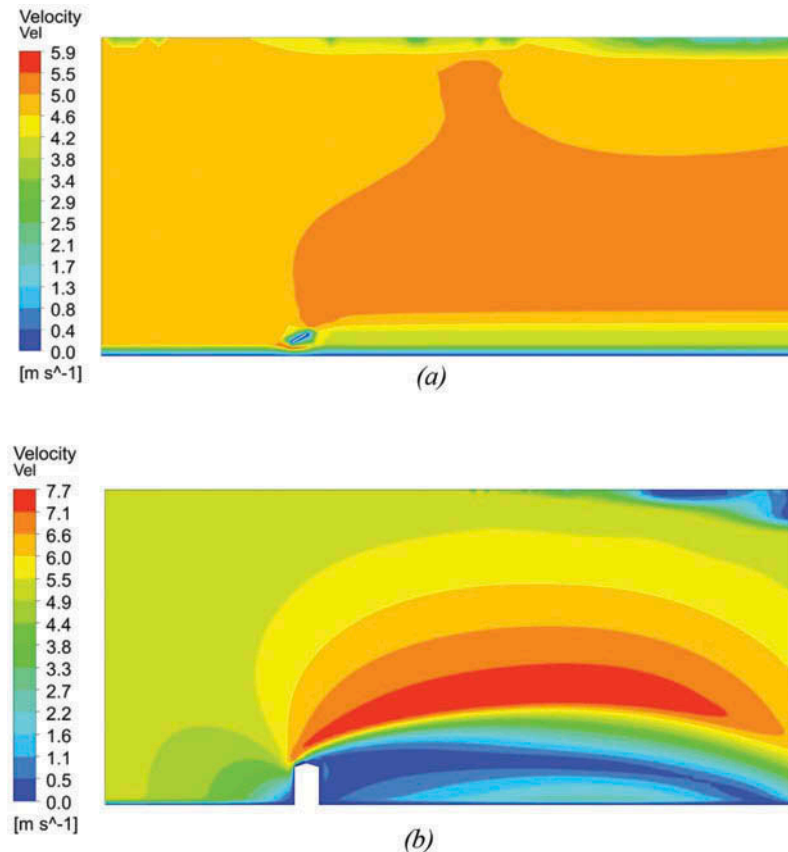
The characteristic wind flow fields near the PV module were used to interpret the soiling rates and the soiling behaviour of the various configurations and particle sizes used. Figure 8 shows the velocity fields on the PV module at varying tilt and azimuth angles. There are complex velocity fields near the PV module caused by the existence of the building and the solar PV module as wind barriers and this phenomenon was also reported elsewhere (Lu & Zhao, 2019).

The velocity fields on the rooftop solar PV array are different from velocity fields for ground-mounted PV module. The velocity variations are more pronounced on roof-mounted PV array

Table 4. Parameter correlation analysis

	Parameter	Relevance	Correlation Value
1	Tilt	0.89	-0.593
2	Orientation	0.76	-0.501
3	Particle size	0.43	-0.124

Figure 8. Wind flow characteristics of ground-mounted and rooftop PV collector. (a) Ground-mounted (30°). (b) Roof-mounted (30°).

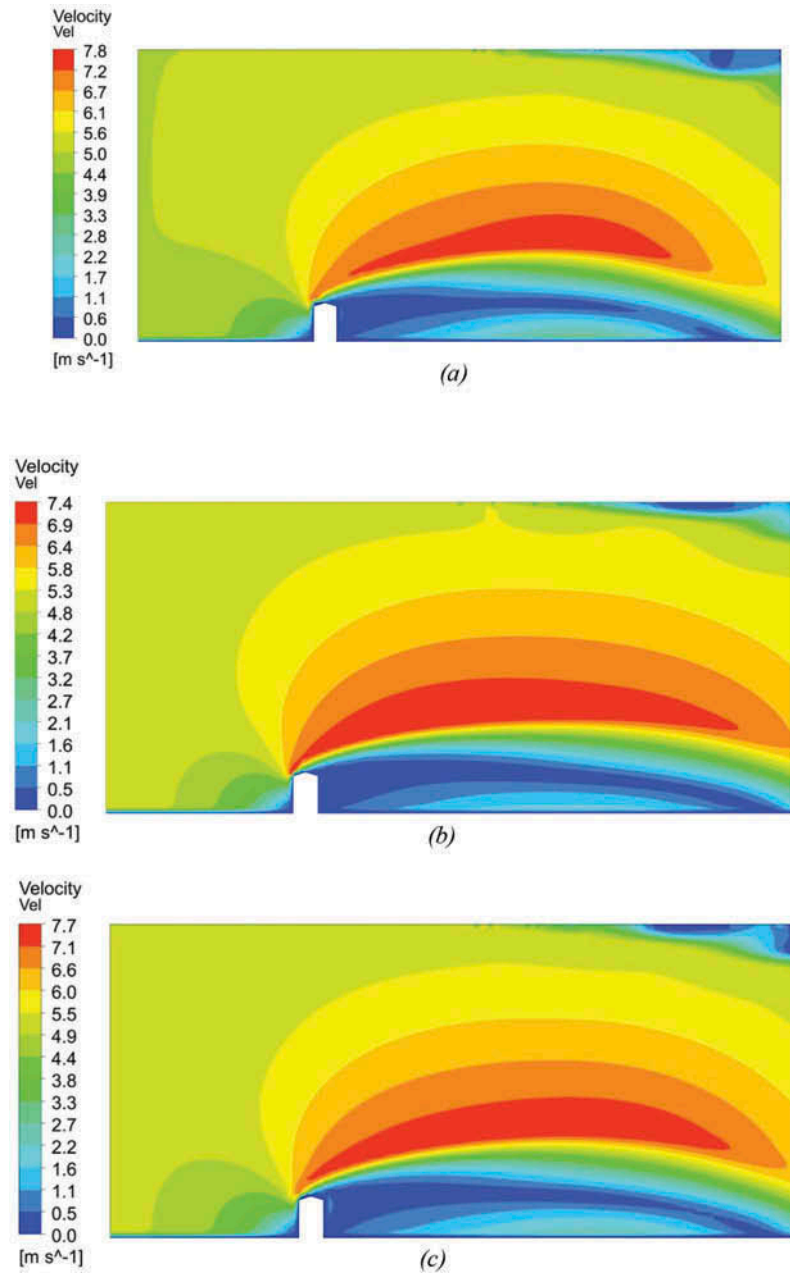


compared to the ground-mounted array. Further, lower impact velocities are experienced on the ground-mounted PV collector compared to the roof-mounted collectors. This is the reason for 11.8% more deposition recorded on the ground-mounted PV collector compared to the roof-mounted PV module. This scenario is due to the effect of surface roughness of the ground which significantly reduces the wind velocity near the ground (Justus & Mikhail, 1976). Frictional resistance affects airflow near the ground surface. The velocity is thus reduced and this phenomenon is known as wind shear (Twidell & Weir, 2015). As previously reported, higher wind velocities tend to reduce deposition compared to lower wind velocities (Maghami et al., 2016; Mani & Pillai, 2010). The significantly more deposition on the ground-mounted PV collectors is attributed to the wider spectrum of impact velocities ranging from 1.8m/s to 3.7m/s. These speeds are more influential on dust deposition for all particles sizes below about 150 μm . On rooftop solar PV collectors, the speed range was a bit narrower (1.6m/s to 2.2m/s) and this limits the number of particles depositing on the solar collectors. This phenomenon agrees well with results obtained by Klinkov et al. (2005).

The velocity fields for the roof-mounted solar collectors shown in Figures 9 and 10 are almost similar for all configurations although some slight differences can be noted which resulted in the differences in particle deposition rates.

Figure 11 shows the Turbulent Kinetic Energy (TKE) profiles which are also almost similar for all configurations like the case for velocity fields for the roof-mounted solar PV collectors. The ground-mounted PV module has lower values of TKE compared to the roof-mounted solar collectors. However, for the ground-mounted PV module, the TKE profile is close to the PV collector compared to the roof-mounted configurations. This occurrence may increase dust deposition on ground-mounted PV collectors due to higher turbulent particle fluctuations near the PV collector surface (Z. Zhang & Chen, 2009).

Figure 9. Velocity fields near the PV collector at an azimuth of 0° with varying tilt angle. (a) 5° (b) 17.5°. (c) 30°.



The velocity streamlines of airflow near the solar PV collector are highlighted in Figure 12. Streamlines represent the path followed by particles suspended in the fluid and they describe flow in terms of velocity and direction. The spacing between the streamlines is inversely proportional to the flow velocity. There are turbulent eddies near the PV module and these occurred behind the installation for all configurations. At 0° azimuth, the turbulent eddies were much closer to the PV module and this had an effect of causing more deposition on 0° azimuth compared to other azimuth angles. The turbulent eddies for 22.5° azimuth were much weaker compared to those at 0° resulting in less deposition compared the 0° azimuth. The 5° tilt angle had apparently larger turbulent eddies compared to the other tilt angles. This could be the reason for more deposition of dust particles (Lu & Zhao, 2019). TKE is related to flow velocity

Figure 10. Similarity of wind velocity profiles for different tilt angles on roof-mounted PV collectors. (a) 30° tilt, 22.5° azimuth. (b) 5° tilt, 0° azimuth.

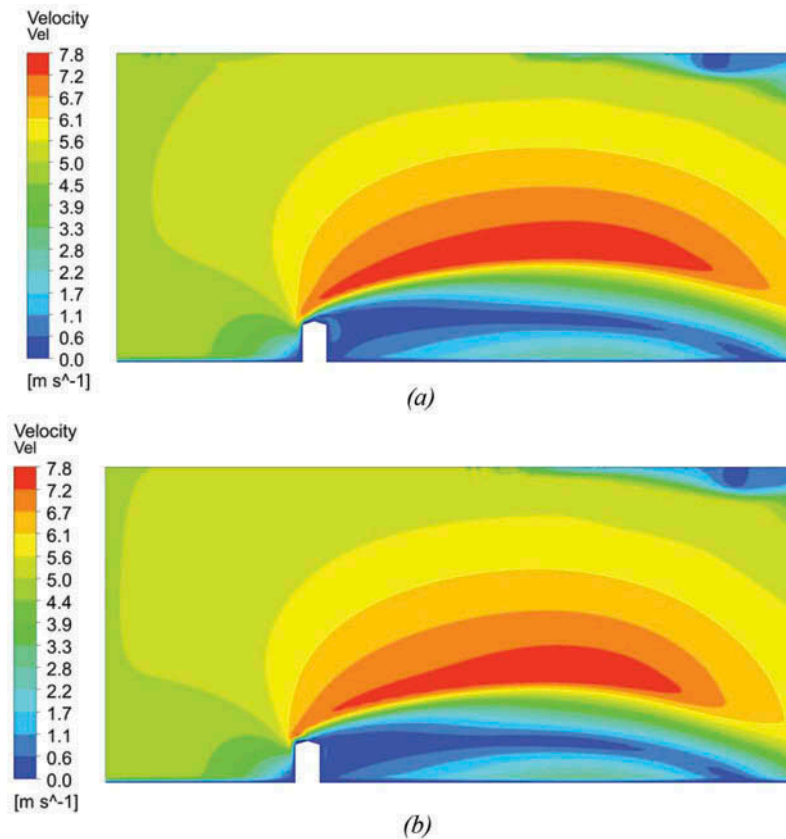
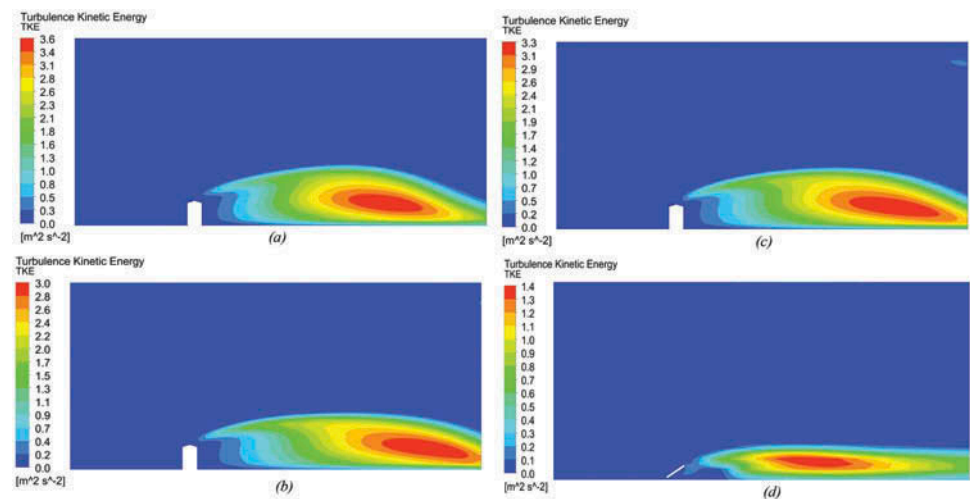


Figure 11. TKE profiles for the three different configurations. (a) 5°. (b) 17.5°. (c) 30°. (d) 30°, ground-mounted.

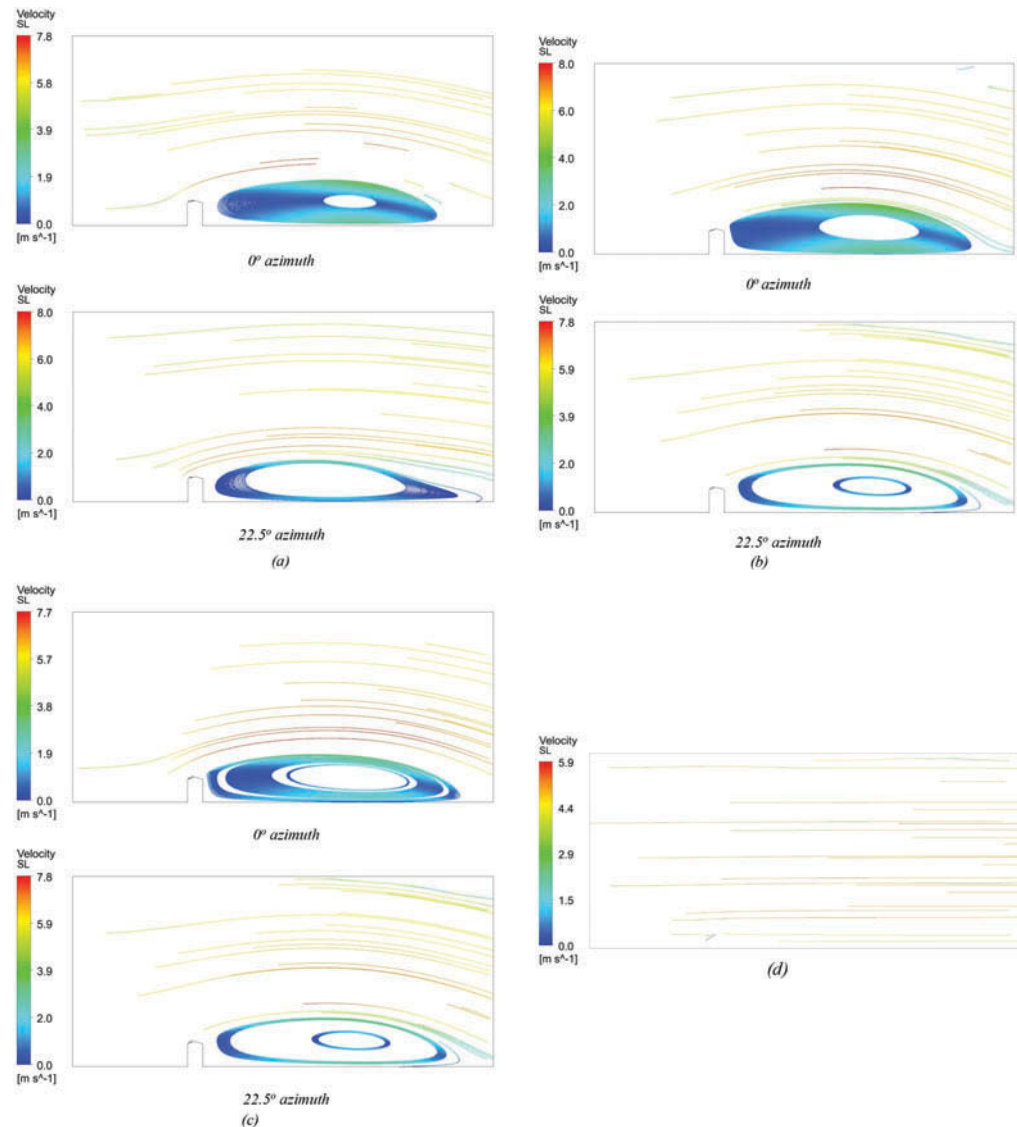


and turbulent eddies and their variations result from the solar PV module inversion (Lu & Zhang, 2019).

4. Conclusions

The study investigated dust deposition phenomenon and turbulent airflow characteristic behaviour on a multi-storey building using a 3-dimensional CFD simulation model. The influence of installation tilt,

Figure 12. Velocity streamlines for the different tilt and azimuth angles.



azimuth and dust particle sizes on soiling was analysed. In this investigation, the following observations were noted:

- The wind flow fields and hence the soiling characteristics are completely different for roof-mounted and ground-mounted PV collectors. Rooftops experience higher wind velocities unlike ground-mounted installations. Ground-mounted installations experience a wider spectrum of impact velocities and hence more deposition is experienced with 11.8% more soiling compared to roof-mounted PV arrays.
- On rooftop installations, there are very small differences on the velocity fields, TKE profiles as well as the velocity streamlines. This is attributed to the relatively larger building height which influences wind flow compared to the PV array size used which has less influence on wind flow compared to the building.
- Tilt and azimuth angles had a significant influence on dust deposition compared to dust particle size. Particle sizes of 100 μm had more deposition at lower impact velocities compared to other particle sizes while lower tilt angles of 5° experienced more soiling.

Nomenclature

δ	Deposition rate (particles/day)
λ	Fitting factor
η_c	Power efficiency without soiling (%)
η_s	Power efficiency with soiling (%)
C_p	Pressure coefficient
U	Wind velocity (m/s)
Re	Particles' Reynolds number
g_i	Gravitational acceleration (m/s ²)
S	Particle to fluid density ratio
d	Diameter (m)
K_ω	Cross-diffusion term.
Γ_k	The effective diffusivity of k
Γ_ω	The effective diffusivity of ω
L_ω	Dissipation rate of ω ;
L_k	Dissipation rate of k
G_k	Generation term for turbulent kinetic energy k (m ² /s ²)
ω	Specific dissipation rate
ρ	Density (kg/m ³)
t	Time (s)
κ	Thermal conductivity (Wm ⁻¹ K ⁻¹)
u	Velocity vector (m·s ⁻¹)
$\Gamma_{\omega,eff}$	Effective diffusion coefficient (m ² /s)
Φ	independent flow variable
S_Φ	source term (kg/m ³ s)
G_ω	generation term for specific dissipation rate ω (s ⁻¹)

Abbreviations

CFD	Computational Fluid Dynamics
PV	Photovoltaic
RANS	Reynolds Averaged Navier-Stokes Equations
(SST) k- ω	Shear Stress Transport k- ω
DPM	Discrete Phase Model
DRW	Discrete Random Walk
FVM	Finite Volume Method
SIMPLE	Semi-Implicit Method for Pressure Linked Equations
RMSE	Residual Mean Square Error
TKE, k	Turbulent Kinetic Energy

Funding

The authors received no direct funding for this research.

Competing Interest

The authors declare no conflict of interest.

Author details

Kudzanayi Chiteka¹
 E-mail: tavakudzira@gmail.com
 ORCID ID: <http://orcid.org/0000-0003-3697-5961>
 S. N. Sridhara²
 E-mail: sridharasn1964@gmail.com
 ORCID ID: <http://orcid.org/0000-0002-4393-6314>

Rajesh Arora²

E-mail: rajesharora1219@gmail.com

ORCID ID: <http://orcid.org/0000-0001-9234-4115>

¹ Department of Industrial and Manufacturing Engineering, Harare Institute of Technology, Belvedere, Harare, Zimbabwe.

² Department of Mechanical Engineering, Amity University Haryana, Gurgaon 122413, India.

Citation information

Cite this article as: Numerical investigation of installation and environmental parameters on soiling of roof-mounted solar photovoltaic array, Kudzanayi Chiteka, S. N. Sridhara & Rajesh Arora, *Cogent Engineering* (2019), 6: 1649007.

References

- Abiola-Ogedengbe, A., Hangan, H., & Siddiqui, K. (2015). Experimental investigation of wind effects on a standalone photovoltaic (PV) module. *Renewable Energy*, 78, 657–665. doi:10.1016/j.renene.2015.01.037
- Adinoyi, M. J., & Said, S. A. M. (2013). Renewable energy. *Effect of Dust Accumulation on the Power Outputs of Solar Photovoltaic Modules*, 60, 633–636. doi:10.1016/j.renene.2013.06.014. Technical note
- Arora, R., & Arora, R. (2018). Experimental investigations and exergetic assessment of 1 kW solar PV plant. *Pertanika Journal of Science & Technology*, 26(4), 1881–1897.
- Arora, R., Arora, R., & Sridhara, S. N. (2019). Performance assessment of 186 kWp grid interactive solar photovoltaic plant in Northern India. *International Journal of Ambient Energy*, 1–28. doi:10.1080/01430750.2019.1630312
- Arora, R., Kaushik, S. C., & Kumar, R. (2016a). Multi-objective thermodynamic optimization of solar parabolic dish Stirling heat engine with regenerative losses using NSGA-II and decision making. *Applied Solar Energy*, 52(4), 295–304. doi:10.3103/S0003701X16040046
- Arora, R., Kaushik, S. C., & Kumar, R. (2017). Multi-objective thermodynamic optimisation of solar parabolic dish Stirling heat engine using NSGA-II and decision making. *International Journal of Renewable Energy Technology*, 8(1), 64–92. doi:10.1504/IJRET.2017.080873
- Arora, R., Kaushik, S. C., Kumar, R., & Arora, R. (2016b). Multi-objective thermo-economic optimization of solar parabolic dish Stirling heat engine with regenerative losses using NSGA-II and decision making. *International Journal of Electrical Power & Energy Systems*, 74, 25–35. doi:10.1016/j.ijepes.2015.07.010
- Chen, C.-Y., Chesnutt, J. K. W., Chien, C. H., Guo, B., & Wu, C.-Y. (2019). Dust removal from solar concentrators using an electrodynamic screen. *Solar Energy*, 187, 341–351. doi:10.1016/j.solener.2019.05.044
- Chiteka, K., Arora, R., & Jain, V. (2019). CFD Prediction of dust deposition and installation parametric optimisation for soiling mitigation in non-tracking solar PV modules. *International Journal of Ambient Energy*, 1–14. doi:10.1080/01430750.2019.1594373
- Connolly, D., Lund, H., Mathiesen, B. V., & Leahy, M. (2010). A review of computer tools for analysing the integration of renewable energy into various energy systems. *Applied Energy*, 87(4), 1059–1082. doi:10.1016/j.apenergy.2009.09.026
- Elminir, H. K., Ghitass, A. E., Hamid, R. H., El-Hussainy, F., Beheary, M. M., & Abdel-Moneim, K. M. (2006). Effect of dust on the transparent cover of solar collectors.

- Energy Conversion and Management*, 47(18–19), 3192–3203. doi:10.1016/j.enconman.2006.02.014
- El-Nashar, A. M. (1994). The effect of dust accumulation on the performance of evacuated tube collectors. *Solar Energy*, 53(1), 105–115. doi:10.1016/S0038-092X(94)90610-6
- El-Shobokshy, M. S., & Hussein, F. M. (1993). Effect of dust with different physical properties on the performance of photovoltaic cells. *Solar Energy*, 51(6), 505–511. doi:10.1016/0038-092X(93)90135-B
- Enkhardt, S. (2018, November 30). *PV info link expects solar demand to reach 112 GW in 2019* (PV Magazine - Photovoltaics Markets and Technology). Retrieved from <https://www.pv-magazine.com/2018/11/30/pv-info-link-expects-solar-demand-to-reach-112-gw-in-2019/>
- Goossens, D., & Kerschaefer, E. V. (1999). Aeolin dust deposition on photovoltaic solar cells: The effects of wind velocity and airborne dust concentration on cell performance. *Solar Energy*, 66, 277–289. doi:10.1016/S0038-092X(99)00028-6
- Goossens, D., Offer, Z. Y., & Zangvil, A. (1993). Wind tunnel experiments and field investigations of eolian dust deposition on photovoltaic solar collectors. *Solar Energy*, 50(1), 75–84. doi:10.1016/0038-092X(93)90009-D
- Guo, B., Javed, W., Khoo, Y. S., & Figgis, B. (2019). Solar PV soiling mitigation by electrodynamic dust shield in field conditions. *Solar Energy*, 188, 271–277. doi:10.1016/j.solener.2019.05.071
- Heggøy, M. W. (2017). *Numerical investigation of particle dispersion in a gravitational field and in zero gravity* (Master of Science Thesis). The University of Bergen, Department of Physics and Technology
- Heydarabadi, H., Abdolzadeh, M., & Lari, K. (2017). Simulation of airflow and particle deposition settled over a tilted photovoltaic module. *Energy*, 139, 1016–1029. doi:10.1016/j.energy.2017.08.023
- Jiang, Y., Lu, L., & Lu, H. (2016). A novel model to estimate the cleaning frequency for dirty solar photovoltaic (PV) modules in desert environment. *Solar Energy*, 140, 236–240. doi:10.1016/j.solener.2016.11.016
- Justus, C. G., & Mikhail, A. (1976). Height variation of wind speed and wind distributions statistics. *Geophysical Research Letters*, 3(5), 261–264. doi:10.1029/GL003i005p00261
- Karava, P., Jubayer, C. M., & Savory, E. (2011). Numerical modelling of forced convective heat transfer from the inclined windward roof of an isolated low-rise building with application to photovoltaic/thermal systems. *Applied Thermal Engineering*, 31(11), 1950–1963. doi:10.1016/j.applthermaleng.2011.02.042
- Kawamoto, H., & Guo, B. (2018). Improvement of an electrostatic cleaning system for removal of dust from solar panels. *Journal of Electrostatics*, 91, 28–33. doi:10.1016/j.elstat.2017.12.002
- Klinkov, S. V., Kosarev, V. F., & Rein, M. (2005). Cold spray deposition: Significance of particle impact phenomena. *Aerospace Science and Technology*, 9(7), 582–591. doi:10.1016/j.ast.2005.03.005
- Kumar, N. M., Sudhakar, K., Samyano, M., & Sukumaran, S. (2018). Dust cleaning robots (DCR) for BIPV and BAPV solar power plants-A conceptual framework and research challenges. *Procedia Computer Science*, 133, 746–754. doi:10.1016/j.procs.2018.07.123
- Lee, H., Wray, T., & Agarwal, R. K. (2016). CFD performance of turbulence models for flow from supersonic nozzle exhausts. *34th AIAA Applied Aerodynamics Conference. Presented at the 34th AIAA Applied Aerodynamics Conference*, Washington, DC. doi:10.2514/6.2016-3433
- Li, X., Dunn, P. F., & Brach, R. M. (2000). experimental and numerical studies of microsphere oblique impact with planar surfaces. *Journal of Aerosol Science*, 31(5), 583–594. doi:10.1016/S0021-8502(99)00544-3
- Liu, S., Pan, W., Cheng, X., Zhang, H., Long, Z., & Chen, Q. (2018). CFD simulations of wind flow in an urban area with a full-scale geometrical model. *4th International conference on building energy, environment, COBEE2018-Paper063*, Melbourne, Australia (pp. 174–179).
- Lu, H., Lu, L., & Wang, Y. (2016). Numerical investigation of dust pollution on a solar photovoltaic (PV) system mounted on an isolated building. *Applied Energy*, 180, 27–36. doi:10.1016/j.apenergy.2016.07.030
- Lu, H., & Zhang, L. (2018). Numerical study of dry deposition of monodisperse and polydisperse dust on building-mounted solar photovoltaic panels with different roof inclinations. *Solar Energy*, 176, 535–544. doi:10.1016/j.solener.2018.10.068
- Lu, H., & Zhang, L.-Z. (2019). Influences of dust deposition on ground-mounted solar photovoltaic arrays: A CFD simulation study. *Renewable Energy*, 135, 21–31. doi:10.1016/j.renene.2018.11.096
- Lu, H., & Zhao, W. (2018). Effects of particle sizes and tilt angles on dust deposition characteristics of a ground-mounted solar photovoltaic system. *Applied Energy*, 220, 514–526. doi:10.1016/j.apenergy.2018.03.095
- Lu, H., & Zhao, W. (2019). CFD prediction of dust pollution and impact on an isolated ground-mounted solar photovoltaic system. *Renewable Energy*, 131, 829–840. doi:10.1016/j.renene.2018.07.112
- Maghami, M. R., Hizam, H., Gomes, C., Radzi, M. A., Rezadad, M. I., & Hajighorbani, S. (2016). Power loss due to soiling on solar panel: A review. *Renewable and Sustainable Energy Reviews*, 59, 1307–1316. doi:10.1016/j.rser.2016.01.044
- Mailu, J. T., Murase, H., & Inoti, I. K. (1994). Knowledge engineering-based studies on solar energy utilization in Kenya. *Agriculture Mechanization in Asia, Africa, and Latin America*, 25, 13–16.
- Mani, M., & Pillai, R. (2010). Impact of dust on solar photovoltaic (PV) performance: Research status, challenges and recommendations. *Renewable and Sustainable Energy Reviews*, 14(9), 3124–3131. doi:10.1016/j.rser.2010.07.065
- Mekhilef, S., Saidur, R., & Kamalisarvestani, M. (2012). Effect of dust, humidity and air velocity on efficiency of photovoltaic cells. *Renewable and Sustainable Energy Reviews*, 16(5), 2920–2925. doi:10.1016/j.rser.2012.02.012
- Mozumder, M. S., Mourad, A. H. I., Pervez, H., & Surkatti, R. (2019). Recent developments in multifunctional coatings for solar panel applications: A review. *Solar Energy Materials and Solar Cells*, 189, 75–102. doi:10.1016/j.solmat.2018.09.015
- Mussard, M., & Amara, M. (2018). Performance of solar photovoltaic modules under arid climatic conditions: A review. *Solar Energy*, 174, 409–421. doi:10.1016/j.solener.2018.08.071
- Pavan, A. M., Mellit, A., De Pieri, D., & Kalogirou, S. A. (2013). A comparison between BNN and regression polynomial methods for the evaluation of the effect of soiling in large scale photovoltaic plants. *Applied Energy*, 108, 392–401. doi:10.1016/j.apenergy.2013.03.023
- Said, S. A. M., Hassan, G., Walwil, H. M., & Al-Aqeeli, N. (2018). The effect of environmental factors and dust accumulation on photovoltaic modules and

- dust-accumulation mitigation strategies. *Renewable and Sustainable Energy Reviews*, 82, 743–760. doi:10.1016/j.rser.2017.09.042
- Sarver, T., Al-Qaraghuli, A., & Kazmerski, L. L. (2013). A comprehensive review of the impact of dust on the use of solar energy: History, investigations, results, literature, and mitigation approaches. *Renewable and Sustainable Energy Reviews*, 22, 698–733. doi:10.1016/j.rser.2012.12.065
- Sayyah, A., Horenstein, M. N., & Mazumder, M. K. (2014). Energy yield loss caused by dust deposition on photovoltaic panels. *Solar Energy*, 107, 576–604. doi:10.1016/j.solener.2014.05.030
- Tanesab, J., Parlevliet, D., Whale, J., & Urme, T. (2019). The effect of dust with different morphologies on the performance degradation of photovoltaic modules. *Sustainable Energy Technologies and Assessments*, 31, 347–354. doi:10.1016/j.seta.2018.12.024
- Tominaga, Y., Akabayashi, S. I., Kitahara, T., & Arinami, Y. (2015). Air flow around isolated gable-roof buildings with different roof pitches: Wind tunnel experiments and CFD simulations. *Building and Environment*, 84, 204–213. doi:10.1016/j.buildenv.2014.11.012
- Twidell, J., & Weir, T. (2015). *Renewable energy resources* (Third ed.). London: Routledge, Taylor & Francis Group.
- Wang, P., Xie, J., Ni, L., Wan, L., Ou, K., Zheng, L., & Sun, K. (2018). Reducing the effect of dust deposition on the generating efficiency of solar PV modules by super-hydrophobic films. *Solar Energy*, 169, 277–283. doi:10.1016/j.solener.2017.12.052
- Williams, S. (n.d.). High rise solar panel cleaning completed in Bromley. Retrieved from <http://www.solar-panel-cleaners.com/high-rise-solar-panel-cleaning-completed-in-bromley>
- Xu, R., Ni, K., Hu, Y., Si, J., Wen, H., & Yu, D. (2017). Analysis of the optimum tilt angle for a soiled PV panel. *Energy Conversion and Management*, 148, 100–109. doi:10.1016/j.enconman.2017.05.058
- Zhang, X. (2009). *CFD simulation of neutral ABL flows* (Risø-R_1688 (EN), 1–40). Risø DTU National Laboratory for Sustainable Energy. Technical University of Denmark, Roskilde, Denmark.
- Zhang, Z., & Chen, Q. (2009). Prediction of particle deposition onto indoor surfaces by CFD with a modified Lagrangian method. *Atmospheric Environment*, 43(2), 319–328. doi:10.1016/j.atmosenv.2008.09.041
- Zhao, B., Zhang, Y., Li, X., Yang, X., & Huang, D. (2004). Comparison of indoor aerosol particle concentration and deposition in different ventilated rooms by numerical method. *Building and Environment*, 39, 1–8. doi:10.1016/j.buildenv.2003.08.002
- Zhu, L., Li, A., & Wang, Z. (2018). Analysis of particle trajectories in a quick-contact cyclone reactor using a discrete phase model. *Separation Science and Technology*, 53(6), 928–939. doi:10.1080/01496395.2017.1386683



© 2019 The Author(s). This open access article is distributed under a Creative Commons Attribution (CC-BY) 4.0 license.

You are free to:

Share — copy and redistribute the material in any medium or format.

Adapt — remix, transform, and build upon the material for any purpose, even commercially.

The licensor cannot revoke these freedoms as long as you follow the license terms.

Under the following terms:

Attribution — You must give appropriate credit, provide a link to the license, and indicate if changes were made.

You may do so in any reasonable manner, but not in any way that suggests the licensor endorses you or your use.

No additional restrictions

You may not apply legal terms or technological measures that legally restrict others from doing anything the license permits.



Cogent Engineering (ISSN: 2331-1916) is published by Cogent OA, part of Taylor & Francis Group.

Publishing with Cogent OA ensures:

- Immediate, universal access to your article on publication
- High visibility and discoverability via the Cogent OA website as well as Taylor & Francis Online
- Download and citation statistics for your article
- Rapid online publication
- Input from, and dialog with, expert editors and editorial boards
- Retention of full copyright of your article
- Guaranteed legacy preservation of your article
- Discounts and waivers for authors in developing regions

Submit your manuscript to a Cogent OA journal at www.CogentOA.com

